in vivo *36*: 1667-1675 (2022)
doi:10.21873/invivo.12878

In Vivo Imaging of Neo-angiogenesis of Transplanted Metastases in Subrenal Capsule Assay Induced Rat Model

JUDIT P. SZABO[1,2], NOEMI DENES[1], VIKTORIA ARATO[1], SZILVIA RACZ[3], ADRIENN KIS[1], GABOR OPPOSITS[1], ZITA KEPES[1], ISTVAN HAJDU[1], ISTVAN JOSZAI[1], MIKLOS EMRI[1], ISTVAN KERTESZ[1], GABOR MEZO[4,5] and GYORGY TRENCSENYI[1,2]

[1]*Division of Nuclear Medicine and Translational Imaging, Department of Medical Imaging, Faculty of Medicine, University of Debrecen, Debrecen, Hungary;*
[2]*Doctoral School of Clinical Medicine, Faculty of Medicine, University of Debrecen, Debrecen, Hungary;*
[3]*Division of Radiology, Department of Medical Imaging, Faculty of Medicine, University of Debrecen, Debrecen, Hungary;*
[4]*Eötvös Loránd University, Faculty of Science, Institute of Chemistry, Budapest, Hungary;*
[5]*MTA-ELTE, Research Group of Peptide Chemistry, Hungarian Academy of Sciences, Eötvös L. University, Budapest, Hungary*

Abstract. *Background/Aim: Changes in the expression of neo-angiogenic molecules in the primary tumor and its metastases may significantly affect the efficacy of therapies. The aim of this study was to evaluate the alterations in aminopeptidase N (APN/CD13) and $\alpha_v\beta_3$ integrin receptor expression in serially transplanted mesoblastic nephroma tumor (Ne/De) metastases using ^{68}Gallium (^{68}Ga)-labeled NOTA-cNGR and NODAGA-RGD radiotracers and preclinical positron emission tomography (PET) imaging. Materials and Methods: Primary and metastatic mesoblastic nephroma (Ne/De) tumors were induced by subrenal capsule assay (SRCA) in Fischer-344 rats. In vivo PET imaging experiments were performed 8±1 days after the SRCA surgery using intravenously injected ^{68}Ga-NOTA-c(NGR), ^{68}Ga-NODAGA-RGD, and [^{18}F]FDG radiotracers. Results: Among the examined neo-angiogenic molecules, the expression of $\alpha_v\beta_3$ integrin in the tumors was significantly lower than that of APN/CD13. This observation was confirmed by the PET data analysis, where a 2-6-fold higher APN/CD13-specific ^{68}Ga-NOTA-cNGR accumulation was observed in both primary malignancies and metastases. However, a steadily increased accumulation of [^{18}F]FDG, ^{68}Ga-NODAGA-RGD, and ^{68}Ga-NOTA-cNGR was observed in the tumors growing under the renal capsule and in the metastatic parathymic lymph nodes during serial transplantations. The observed increase in ^{68}Ga-NOTA-cNGR accumulation during serial transplantations correlated well with the western blot analysis, where APN/CD13 protein levels were also elevated in the metastatic parathymic lymph nodes. Conclusion: The observed increase in glucose metabolism and the up-regulated expression of $\alpha_v\beta_3$ integrin and APN/CD13 during serial transplantations of metastases may indicate enhanced malignancy.*

Correspondence to: György Trencsényi, Division of Nuclear Medicine and Translational Imaging, Department of Medical Imaging, Faculty of Medicine, University of Debrecen, Nagyerdei krt. 98, Debrecen 4032, Hungary. Tel: +36 52255000/56194, Fax: +36 52255500/56436, e-mail: trencsenyi.gyorgy@med.unideb.hu

Key Words: Aminopeptidase N, angiogenesis, ^{68}Ga-NOTA-c(NGR), metastasis, NGR peptide, positron emission tomography.

Malignant diseases and their metastases represent an ever increasing serious health concern worldwide (1). Both preclinical and clinical studies accomplished in recent years have widen our understanding of the multi-step process of metastatic cascade, however, it remains an open question whether metastases metastasize or all of them derive from the primary lesion, and whether this process can be followed by detecting changes in the expression of cell surface molecules in metastases. Accordingly, exact knowledge of the changes in the molecular expression pattern of the metastases would not only ensure accurate lesion detection but may also lead to the reconsideration of existing therapeutic regimes.

Since angiogenesis is considered to be the cornerstone of tumor progression and metastasis, non-invasive molecular imaging techniques targeting neo-angiogenic mediators/molecules expressed on the surface of cells in metastases and primary tumors may provide a precious diagnostic opportunity for the timely assessment of neoplastic alterations, as well as

for the introduction of strategies to inhibit or decelerate tumor progression (2). Moreover, non-invasive visualization of the molecular hallmarks of neoangiogenesis such as different types of integrins, vascular endothelial growth factor (VEGF), ephrins, or aminopeptidase N (APN/CD13) grants a possibility for anti-angiogenic treatment, follow-up, and accurate therapeutic decisions that have pivotal role in patient management (3). The interaction between VEGF and VEGFR promotes proliferation and migration of the endothelial cells, and the remodeling of the capillary system (4). Therefore, over-expression of VEGF and its receptors (VEGFR) is associated with tumor progression, metastatic potential, microvascular density and poor patient prognosis (5). Since integrin $\alpha_v\beta_3$ promotes tumor and endothelial cell migration, previous studies have pinpointed its critical role in regulating tumor growth, invasiveness and metastasis (6-8). In addition, APN/CD13 has also shown strong connection with tumor-related neo-angiogenesis (9).

PET imaging seems to be a valuable tool for detecting specific molecular biomarkers of neo-angiogenesis opening a novel field towards the deeper understanding of the cell surface molecular pattern of primary tumors and their metastases. In this respect, integrin $\alpha_v\beta_3$ represents an area of increasing preclinical and human clinical research (10). Owing to the up-regulation of $\alpha_v\beta_3$ integrins in tumor tissues, integrin-specific radiolabeled RGD (Arg-Gly-Asp) peptides have crucial role in molecular oncological imaging. Based on its receptor-specific tumor accumulation and favorable elimination kinetics, recent studies conducted in murine tumor models and in humans revealed the feasibility of [^{18}F]Galacto-RGD peptides in the detection of $\alpha_v\beta_3$ expression and quantification (3). In one study, DOTA-conjugated RGD peptide (DOTA-RGDfK) radiolabeled with either ^{111}In or ^{68}Ga has shown similar internalization and uptake values to those of [^{18}F]Galacto-RGD in an $\alpha_v\beta_3$-positive melanoma M21 model (11). Owing to the high binding affinity of NGR (Asn-Gly-Arg) peptide ligands to APN/CD13, administration of medications to the cancerous lesions *via* APN makes the inhibition of angiogenesis possible (12). Comparative analysis of NGR and RGD peptides revealed that the accumulation of ^{68}Ga-NOTA-cNGR was more significant than the uptake of ^{68}Ga-NODAGA-RGD in primary tumors. In addition, [^{18}F]FDG is considered to be an indirect valuable prognostic biomarker for the detection of tumor-related angiogenesis. The above mentioned research findings inspired us to evaluate the expression of neo-angiogenic $\alpha_v\beta_3$ integrin and APN/CD13 expression based on a predefined guideline described by Trencsényi *et al*. applying PET imaging in a rat model in which metastases could be properly followed (13). In the present study, we aimed at examining whether the use of [^{18}F]FDG, ^{68}Ga-NODAGA-RGD and ^{68}Ga-NOTA-cNGR molecules could help us detect serially transplanted mesoblastic nephroma tumor (Ne/De) metastases. Furthermore, we aimed to investigate the alterations in angiogenic molecule expression after sequential transplantation of metastatic parathymic lymph nodes using non-invasive PET imaging.

Materials and Methods

Experimental animals. Sixteen weeks old and 250±20 g weighted female Fischer-344 (n=30) rats were used in this study. Animals were kept in a conventional animal house at controlled temperature (26˚C±2˚C) and humidity (51±10%). Artificial lighting was provided in automatically controlled 12-h circadian cycles. The rats were fed *ad libitum* with semi synthetic feed (Animalab, Budapest, Hungary) and tap water. The experiments were performed in compliance with the criteria of the Ethics Committee for Animal Experimentation of the United Kingdom with the permission of the Ethics Committee for Animal Experimentation of the University of Debrecen (approval number: 21/2017/DEMÁB).

Ne/De tumor. The mesoblastic nephroma (Ne/De) tumor model used in the present study was established by a previous research at the University of Debrecen (14). Briefly, Fischer-344 rats were intraperitoneally injected with 125 μg n-nitrosodimethylamine (Merck, Darmstadt, Germany) saline solution. Approximately after six months the chemically induced Ne/De tumors were removed, and a cell line was established (13).

Culturing of Ne/De cells. Dulbecco's Modified Eagle Medium (DMEM, Merck) containing 10% of foetal bovine serum (FBS, Merck) was used for cell cultivation supplemented with 100 unit/ml penicillin and 100 mg/ml streptomycin (Merck). Monolayer cell cultures were maintained in incubators with 5% CO_2 at 37˚C, and 95% humidity. The passage of the cultures was performed 3 times a week.

Subrenal capsule assay (SRCA) surgery. Rats were anaesthetized before the surgery using 1.5% Forane, (AbbVie, Budapest, Hungary; OGYI-T-1414/01), 0.4 l/min O_2 (Linde Healthcare, Budapest, Hungary; OGYI-T-20607), and 1.2 l/min N_2O (Linde Healthcare; OGYI-T-21090) using an isoflurane anesthesia chamber. The fur off the lumbar region one fingerbreadth under the ribs on the left was shaved, and the area was disinfected. Following the incision of the skin in this area, the muscle layer was intersected to reach the left kidney. The uncovered kidney was continuously moisturized with physiological saline solution. Utilizing Iris scissors a tiny hole was performed on the capsule renalis, through which 1×10^6 Ne/De cells placed on Gelapson disk (Bausch & Lomb, Vaughan, Canada) in 10 μl physiological saline solution (0.9% NaCl solution) were implanted under the renal capsule of the experimental animals. In further studies, 8±1 days after the implantation of the tumor cells, the thoracic parathymic metastatic lymph node was further implanted under the renal capsule of a healthy Fischer-344 rat (Figure 1). The muscle layer was then sutured, and the skin layer was closed with surgical staples. After the surgery a non-steroid anti-inflammatory analgesic containing ibuprofen (Nurofen syrup 10 mg/kg) was administered in drinking water ad libitum (14).

Radiopharmaceuticals. [^{18}F]FDG is routinely produced in the Department of Nuclear Medicine (University of Debrecen, Debrecen, Hungary) with the purpose of examining patients with oncological diseases. Radiochemical production and quality control of APN/CD13 specific ^{68}Ga-NOTA-cNGR and the $\alpha_v\beta_3$ specific ^{68}Ga-NODAGA-RGD was performed as previously described (15, 16).

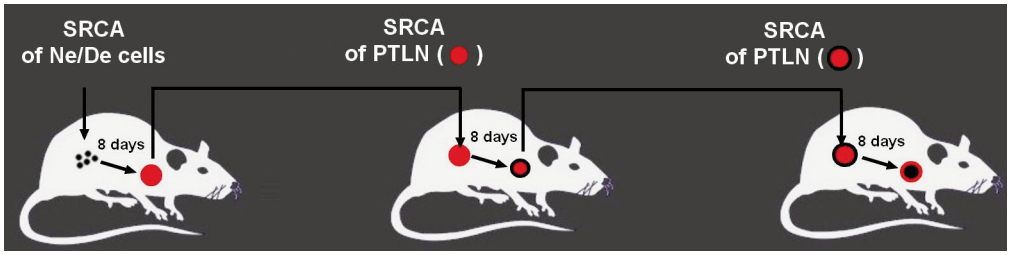

Figure 1. *Schematic diagram of the serial subrenal capsule assay (SRCA) transplantations. PTLN: metastatic parathymic lymph node.*

In vivo PET imaging. Small animal PET imaging was accomplished in the preclinical laboratory of the University of Debrecen, Faculty of Medicine, Department of Clinical Imaging, and Division of Nuclear Medicine. Eight±1 days after the SRCA operation the primary tumors under the renal capsule and the metastatic parathymic lymph nodes in the thorax of the experimental animals were investigated under inhalation anesthesia (1.5% Isoflurane) using intravenously injected [^{18}F]FDG, ^{68}Ga-NODAGA-RGD and ^{68}Ga-NOTA-cNGR radiopharmaceuticals (0.15 ml, approx. 7 MBq in physiological saline solution). Fifty min ([^{18}F]FDG) and 90 min (^{68}Ga-labelled radiotracers) after radiotracer injection, static PET images (20 min/bed position; thoracic regions and the renal areas) were acquired using the MiniPET-II scanner.

Image analysis and data processing. Data derived from the detectors were transferred to the data collecting computer through 100BASE-TX Ethernet channel. 2D ML-EM iterative data reconstruction was carried out and data were stored in MultiModal Medical Imaging Software library. The reconstructed images were evaluated using BrainCAD image processing software. The radiopharmaceutical accumulation was determined by Standardized Uptake Value (SUV). SUV=[VOI activity (Bq/ml)]/[injected activity (Bq)/animal weight (g)], assuming a density of 1 g/m. Tumor-to-muscle (T/M) ratios were calculated from the concentration of the radioactivity in the tumor and the background (skeletal muscle from the scapular region).

Western blot analysis. Ne/De tumors were placed in subtitled Eppendorf tubes in 1 ml PBS, then homogenized, and the supernatant was used for lysis with RIPA buffer (50 mM Tris, 150 mM NaCl, 0.1% SDS, 1% TritonX 100, 0.5% sodium-deoxycholate, 1 mM EDTA, 1 mM Na_3VO_4, 1 mM NaF) supplemented with 1 mM PMSF protease inhibitor (Life Technologies, Budapest, Hungary). The protein content of the samples was measured with Pierce BCA reagent (Thermo Fisher Scientific, Waltham, MA, USA). Molecular weight based (10 μg) separation of proteins was carried out on 10% polyacrylamide gel (Thermo Fisher Scientific), then the protein bands were blotted to nitrocellulose membranes (Bio-Rad, Hercules, CA, USA). Non-specific binding was then blocked with 1xTBS-Tween buffer containing 5% of BSA for 1 h at room temperature, which was followed by the labelling with primary antibody overnight at 4˚C (CD13; Santa Cruz, Heidelberg, Germany; 1:1,000 dilution). After washing with 1×TBS-Tween solution, the membranes were incubated for 1 h at room temperature with anti-mouse secondary antibody conjugated with peroxidase (1:2,000, Cell Signaling Technology, Beverly, MA, USA). Finally, the membranes were washed twice for 10 min in TBS-Tween buffer, and once for 10 min in TBS. Antibody-labeled bands were detected applying chemiluminescent reaction (SuperSignal West Pico Solutions, Thermo Fisher Scientific) with ChemiDoc Touch Imaging gel documentation system (BioRad). The Intensity of the bands was determined with Image Lab 5.2.1 software (BioRad).

Statistical analysis. Data shown on the charts are the results of at least three independent series of measurements presented as mean±SD. Student's two-tailed *t*-test, two-way ANOVA, and the Mann-Whitney rank-sum tests were used for determining significance. The significance level was set at $p<0.05$, and the commercial software package MedCalc 18.5 (MedCalc Software, Mariakerke, Belgium) was used for all statistical analyses.

Results

Evaluation of primary Ne/De tumor and metastases using radiopharmaceuticals. In the first part of the study, primary tumor-forming ability and metastasis of Ne/De cells transplanted under the renal capsule were assessed using *in vivo* PET imaging and [^{18}F]FDG radiotracer. Furthermore, $\alpha_v\beta_3$ integrin and APN/CD13 expression in the primary tumors and their metastases was investigated using ^{68}Ga-NODAGA-RGD and ^{68}Ga-NOTA-cNGR radiopharmaceuticals. After the qualitative analyses of the decay-corrected PET images, we found that the primary Ne/De tumors developing under the renal capsule were well identified using all of the three radiotracers, even though lower tracer uptake was detected in the case of ^{68}Ga-NODAGA-RGD (Figure 2A, black arrows). The thoracic parathymic lymph node metastases were only visible with [^{18}F]FDG and ^{68}Ga-NOTA-cNGR; using ^{68}Ga-NODAGA-RGD these metastases were hardy recognizable (Figure 2B, red arrows). The qualitative observations were confirmed by the quantitative SUV data analysis of the PET images. 8±1 days after the transplantation of Ne/De cells the [^{18}F]FDG uptake of the primary tumors growing under the renal capsule was the highest (SUV_{mean}: 7.25±2.62; SUV_{max}: 14.82±3.21), followed by ^{68}Ga-NOTA-cNGR uptake referring to APN/CD13 expression (SUV_{mean}: 4.12±0.56; SUV_{max}: 10.72±1.85), and the accumulation of the $\alpha_v\beta_3$ integrin specific ^{68}Ga-NODAGA-RGD (SUV_{mean}: 2.05±0.45; SUV_{max}: 5.77±1.08) (Figure 2C). By analyzing the radiotracer accumulation in the metastatic parathymic lymph nodes in the thorax we found similar, but lower uptake values. The [^{18}F]FDG uptake (SUV_{mean}:

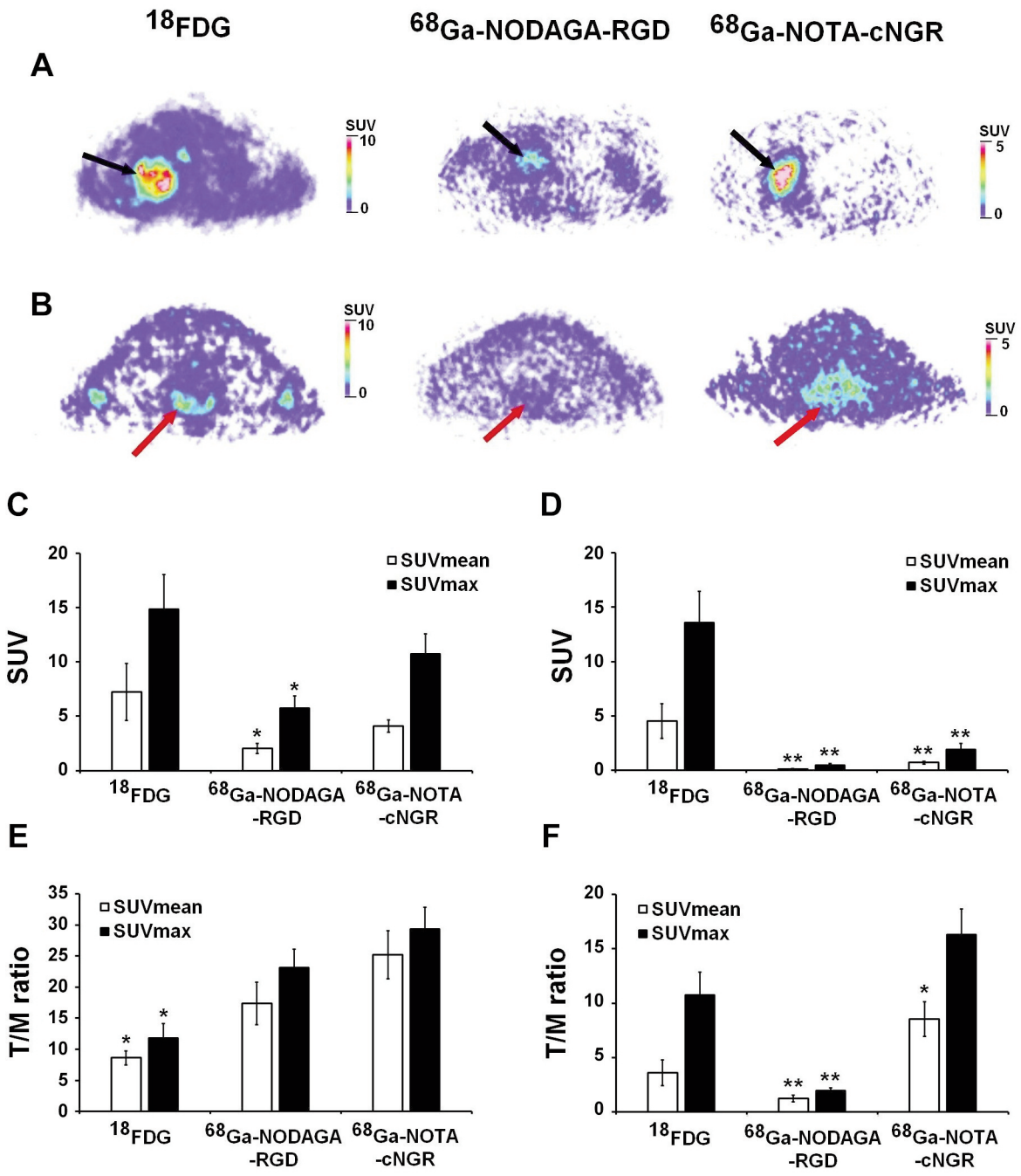

Figure 2. *In vivo PET studies of Ne/De tumor-bearing rats 8±1 days after the SRCA implantation of cancer cells. Representative decay corrected transaxial PET images of primary Ne/De tumors located under the renal capsule (A) and metastatic parathymic lymph nodes in the thorax (B) 50 min after the intravenous injection of [^{18}F]FDG and 90 min after intravenous injection of ^{68}Ga-labelled radiotracers. Quantitative SUV analysis of radiotracer accumulation in the subrenal Ne/De tumors (C and E) and metastatic parathymic lymph nodes (D and F). Black arrows: primary Ne/De tumor, red arrows: parathymic lymph nodes. SUV: standardized uptake value. T/M: tumor-to-muscle ratio. Significance levels: p≤0.05 (*) and p≤0.01 (**). Data is presented as mean±SD; n=3 rats/radiotracer.*

4.53±1.58; SUV_{max}: 13.58±2.89) was significantly higher (at $p \leq 0.01$) than the accumulation of the ^{68}Ga-labelled radiotracers. The ^{68}Ga-NOTA-cNGR (SUV_{mean}: 0.72±0.12; SUV_{max}: 1.92±0.58) accumulation in the parathymic lymph nodes was significantly higher (at $p \leq 0.01$) than that of ^{68}Ga-NODAGA-RGD (SUV_{mean}: 0.11±0.08; SUV_{max}: 0.46±0.15) (Figure 2D).

During the measurement of tumor-to-background ratio (T/M ratio) – which influences the interpretation of the PET images – we found that the primary Ne/De malignancies showed significantly higher (at $p \leq 0.05$) ^{68}Ga-NOTA-cNGR and ^{68}Ga-NODAGA-RGD tracer uptake than the [^{18}F]FDG accumulation (Figure 2E), whereas in the case of metastatic lymph node metastases, high-contrast PET imaging was obtained using [^{18}F]FDG and ^{68}Ga-NOTA-cNGR (Figure 2F).

Investigation of secondary Ne/De tumors and their metastases with radiotracers. In the second part of our study, metastatic parathymic lymph nodes were implanted under the renal capsule of F-344 rats. Eight ±1 days after the SRCA transplantation the primer tumor forming capability, the metastasis and the $\alpha_v\beta_3$ and APN/CD13 expression of the primary malignancies and their metastases were assessed using *in vivo* PET imaging. During the evaluation of decay-corrected PET images in the second series of the experiments, we also observed that the primary Ne/De tumors growing under the renal capsule were obviously recognizable with all radiotracers, however, lower radiopharmaceutical accumulation was detected in the case of ^{68}Ga-NODAGA-RGD (Figure 3A, black arrows). In this part of the experiments the thoracic parathymic lymph node metastases were also unequivocally identifiable using [^{18}F]FDG and ^{68}Ga-NOTA-cNGR (Figure 3B, red arrows). These visual findings were verified by the quantitative SUV data analysis of the PET images (Figure 3C-F). [^{18}F]FDG uptake of the tumors growing under the renal capsule was the highest 8±1 days after the transplantation of the metastatic lymph node (SUV_{mean}: 8.56±2.58; SUV_{max}: 16.25±3.41). This was followed by the APN/CD13 specific ^{68}Ga-NOTA-cNGR (SUV_{mean}: 5.23±0.89; SUV_{max}: 11.41±2.21), and lastly by the $\alpha_v\beta_3$ targeting ^{68}Ga-NODAGA-RGD (SUV_{mean}: 2.85±0.52; SUV_{max}: 6.49±1.12). Lower SUV values were determined regarding thoracic parathymic lymph node metastases, where the [^{18}F]FDG accumulation was the highest (SUV_{mean}=5.36±1.69 and SUV_{max}=14.75±3.08). ^{68}Ga-NOTA-cNGR (SUV_{mean}: 0.99±0.15; SUV_{max}: 2.09±0.49) uptake was significantly higher (at $p \leq 0.01$) compared to that of ^{68}Ga-NODAGA-RGD (SUV_{mean}: 0.23±0.14; SUV_{max}: 0.63±0.15) (Figure 3D). Corresponding to the previous series of the experiments, higher tumor-to-background ratio was obtained using ^{68}Ga-NOTA-cNGR and ^{68}Ga-NODAGA-RGD in the case of Ne/De tumors developing from the metastasis compared to [^{18}F]FDG (Figure 3E). However, as for the thoracic metastatic lymph nodes, better visualization in the PET images was obtained with [^{18}F]FDG and ^{68}Ga-NOTA-cNGR (Figure 3F).

Assessment of tercier Ne/De tumors and their metastases with radiotracers. In the third part of our study, thoracic parathymic lymph nodes with metastatic Ne/De cancerous cells derived from the previous series of research were implanted under the renal capsule of the rats, and we assessed the development of the tumor growing under the renal capsule using *in vivo* PET imaging. In addition, metastasis and $\alpha_v\beta_3$ integrin and APN/CD13 expression in the tumors were also investigated. In this series of experiments, we observed similar results to those of the previous ones (the Ne/De tumor growing under the renal capsule was undoubtedly identified with all radiotracers). Lower accumulation was revealed with ^{68}Ga-NODAGA-RGD (Figure 4A, black arrows). We visualized the thoracic parathymic lymph node metastasis with all radiopharmaceuticals in this part of the study (Figure 4B, red arrows). Figure 4 (C-F panels) demonstrates quantitative PET data that supports our visual assessment. 8±1 days after the transplantation, [^{18}F]FDG uptake of the renal tumor was the highest (SUV_{mean}: 9.63±2.66; SUV_{max}: 17.56±3.52), followed by APN/CD13 specific ^{68}Ga-NOTA-cNGR uptake (SUV_{mean}: 6.35±1.09; SUV_{max}: 12.45±2.36) and the $\alpha_v\beta_3$ integrin specific ^{68}Ga-NODAGA-RGD accumulation (SUV_{mean}: 3.35±0.63; SUV_{max}: 7.09±1.35). Lower SUV values of the thoracic parathymic lymph node metastases were registered in that part of the experiment as well. [^{18}F]FDG uptake proved to be the highest with SUV_{mean}=6.33±1.70 and SUV_{max}=15.23±3.21, respectively. Comparing ^{68}Ga-NOTA-cNGR (SUVmean: 1.56±0.20; SUVmax: 2.78±0.51) and ^{68}Ga-NODAGA-RGD (SUVmean: 0.56±0.12; SUVmax: 0.88±0.14) accumulation, the former showed elevated uptake (Figure 4D). As for Ne/De tumors developing from the metastasis, tumor-to-background ratio showed significantly ($p \leq 0.05$) higher values in the case of ^{68}Ga-NOTA-cNGR and ^{68}Ga-NODAGA-RGD compared to [^{18}F]FDG (Figure 4E). However, Figure 4 panel F demonstrates, that thoracic metastatic lymph nodes were more visible using [^{18}F]FDG and ^{68}Ga-NOTA-cNGR.

Quantitative PET and western blot analysis of parathymic lymph nodes. Summarizing the results of the three series of transplantation experiments, we found that the SUV values of the metastatic parathymic lymph nodes increased for all three radiopharmaceuticals, however, the differences were not significant (at $p \leq 0.05$). Taking into account that we were particularly interested in evaluating of the changes in the expression of APN/CD13 neo-angiogenic molecule in the metastatic lymph node, we only focused on this area during protein analysis. Steadily increasing ^{68}GaNOTA-cNGR accumulation in the thoracic metastases was observed during serial transplantations (Figure 5A). This observation was confirmed by western blot analysis, where the amount of APN/CD13 protein was also found to be increased in the metastatic parathymic lymph nodes (Figure 5B).

Discussion

Metastases are considered to be the major cause of cancer mortality. Recent preclinical and clinical research have further our understanding regarding the process of metastatic cascade,

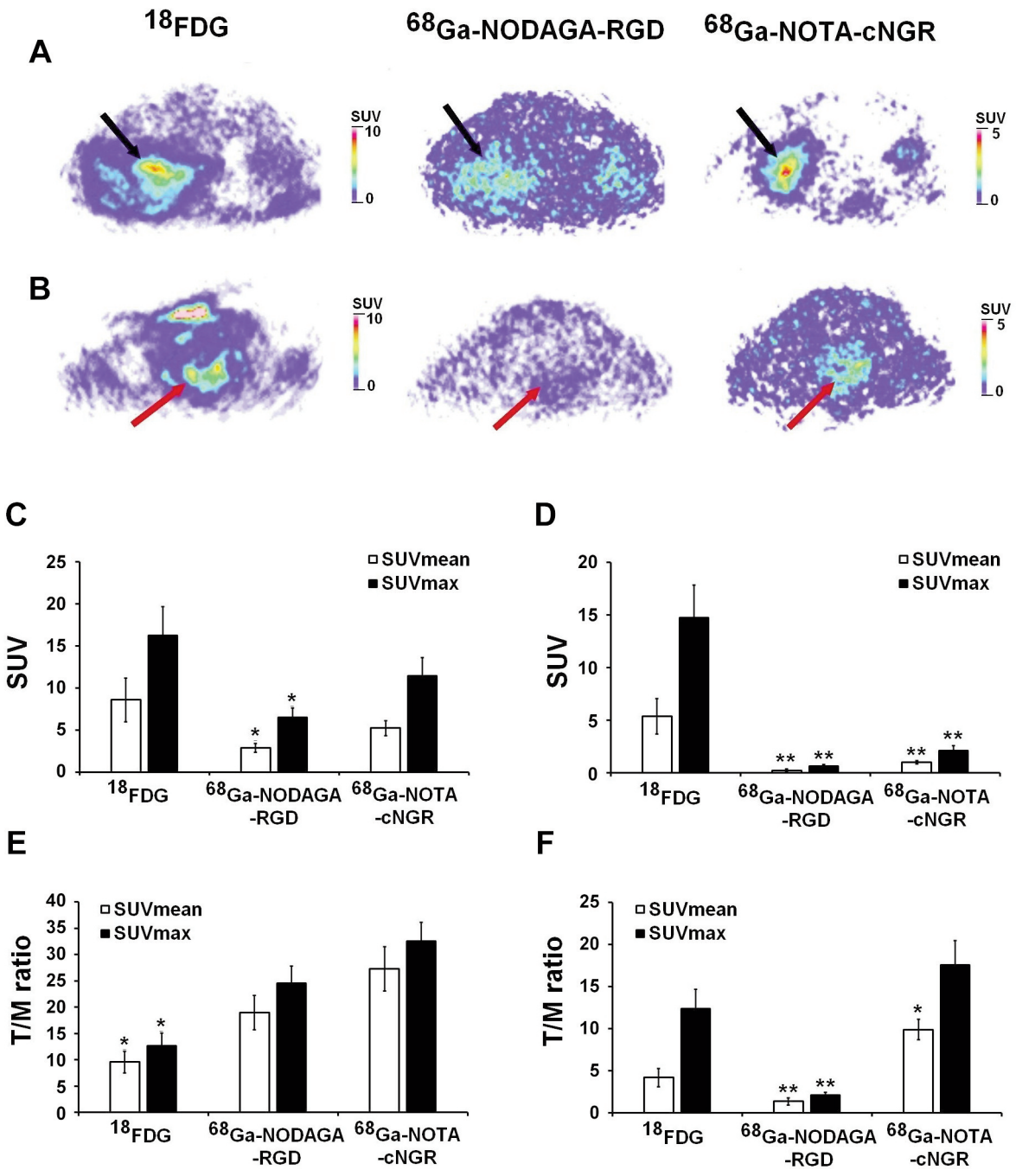

Figure 3. *In vivo PET imaging studies of Ne/De tumor-bearing rats 8±1 days after the SRCA implantation of metastatic parathymic lymph node from the first experiment. Representative decay corrected transaxial PET images of primary Ne/De tumors located under the renal capsule (A) and metastatic parathymic lymph nodes in the thorax (B) 50 min after the intravenous injection of [^{18}F]FDG and 90 min after intravenous injection of ^{68}Ga-labelled radiotracers. Quantitative SUV analysis of radiotracer accumulation in the subrenal Ne/De tumors (C and E) and metastatic parathymic lymph nodes (D and F). Black arrows: primary Ne/De tumor, red arrows: parathymic lymph nodes. SUV: standardized uptake value. T/M: tumor-to-muscle ratio. Significance levels: p≤0.05 (*) and p≤0.01 (**). Data is presented as mean±SD; n=3 rats/radiotracer.*

however, whether metastases develop new metastatic lesions or all metastases derive from the primary lesion still remains unresolved. Based on the existing literature, limited amount of data supports or disproves the metastatic potential of metastases. However, cancerous subpopulations undergo continuous development and change. Therefore, cells with

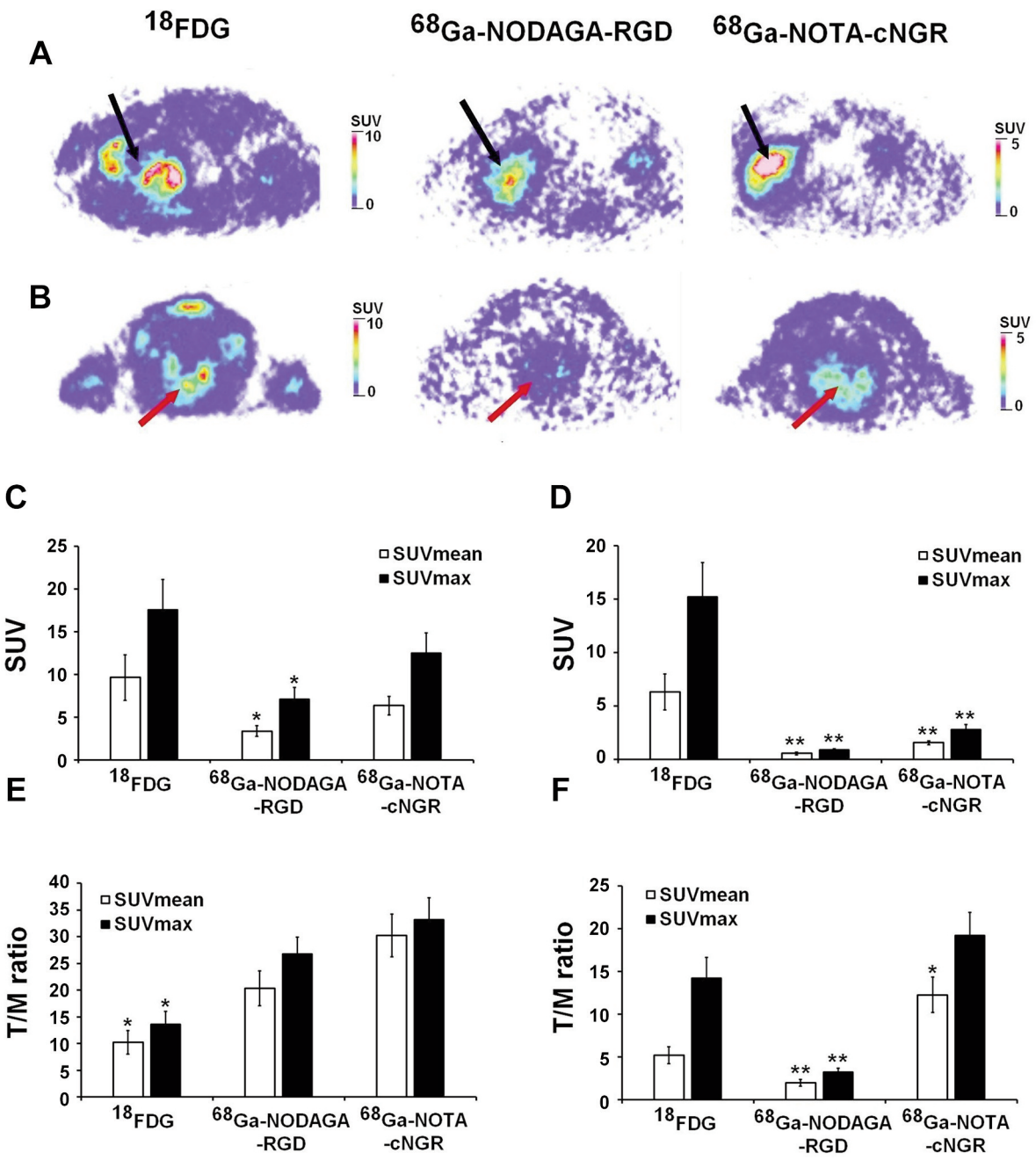

Figure 4. *In vivo PET imaging studies of Ne/De tumor-bearing rats 8±1 days after the SRCA implantation of metastatic parathymic lymph node from the second experiment. Representative decay corrected transaxial PET images of primary Ne/De tumors located under the renal capsule (A) and metastatic parathymic lymph nodes in the thorax (B) 50 min after the intravenous injection of [^{18}F]FDG and 90 min after intravenous injection of ^{68}Ga-labelled radiotracers. Quantitative SUV analysis of radiotracer accumulation in the subrenal Ne/De tumors (C and E) and metastatic parathymic lymph nodes (D and F). Black arrows: primary Ne/De tumor, red arrows: parathymic lymph nodes. SUV: standardized uptake value. T/M: tumor-to-muscle ratio. Significance levels: p≤0.05 (*) and p≤0.01 (**). Data is presented as mean±SD; n=3 rats/radiotracer.*

increasing metastatic potential are formed that are capable of giving metastases to various distant localizations. However, metastatic cells may also undergo changes leading to the loss of their metastatic potential. This may depend on both the type of the tumor and the length of the resting stage period prior to macrometastasis progression. Without convincing research data, drawing final conclusions is difficult. Moreover, the question of metastatic potential of metastases is of clinical

significance from the point of view of therapeutic decision. If this phenomenon is characteristic of particular tumor types, then the identification and treatment of these metastases make the inhibition of the progression of the neoplasm possible. Another unelucidated question is whether the expression pattern of cell surface proteins of the metastases is identical to that of the primary tumor (17, 18).

Hypoxia and hypoxia triggered angiogenesis are notable factors in the induction of metastasis of neoplasms. During our research, the extent of the expression of neo-angiogenic $\alpha_v\beta_3$ integrin and APN/CD13 were evaluated applying *in vivo* PET imaging in a syngeneic rat model where the process of metastasis can be followed. The applied rat model was previously described by Trencsényi *et al.* (13). The found that if cancerous cells or fragments of tumors are transplanted under the renal capsule of the rats, metastasis is formed in the thoracic parathymic lymph node in all cases. This model is termed as lymphatic spreading „skip" metastatic model. As no *in vivo* tumor model is currently available to examine whether metastases form a metastasis, sequential transplantation of metastases may be used (Figure 1). In our opinion, the renal capsule-parathymic lymph node complex can be a suitable model for the study of metastases generating from metastases and their receptor expression.

Primary Ne/De tumors growing under the renal capsule and the thoracic parathymic lymph node metastases developed were well identified using [^{18}F]FDG (as demonstrated in Figure 2, Figure 3, and Figure 4). Based on the above detailed model our team previously identified the feasibility of ^{68}Ga-labelled RGD and NGR peptides utilizing *in vivo* PET imaging in the detection of neo-angiogenesis and the expression of $\alpha_v\beta_3$ integrin and APN/CD13 (15). In the present study we found that the expression of both $\alpha_v\beta_3$ integrin and APN/CD13 in Ne/De chemically induced mesoblastic nephroma tumors and their metastases were recognizable – albeit to a different extent - with ^{68}Ga-NODAGA-RGD and ^{68}Ga-NOTA-cNGR radiotracers in the preclinical PET studies.

Among the investigated angiogenic molecules, the expression of integrin $\alpha_v\beta_3$ was lower in all cases compared to that of APN/CD13 both regarding the primary malignancies and the metastases. This is in line with previous observations, according to which lower tracer uptake was observed in the case of ^{68}Ga-labelled RGD (15, 19).

However, continuous increase of the accumulation of ^{18}FDG, ^{68}Ga-NODAGA-RGD and ^{68}Ga-NOTA-cNGR in the tumors growing under the renal capsule and the thoracic metastasis could be observed during serial transplantations. We may draw the conclusion that the observed increase in glucose metabolism and the up-regulated expression of $\alpha_v\beta_3$ integrin and APN/CD13 molecules associated with neo-angiogenesis, which was observed in case of tumors and their metastases during the serial transplantations of the metastases, may indicate enhanced malignancy (Figure 5).

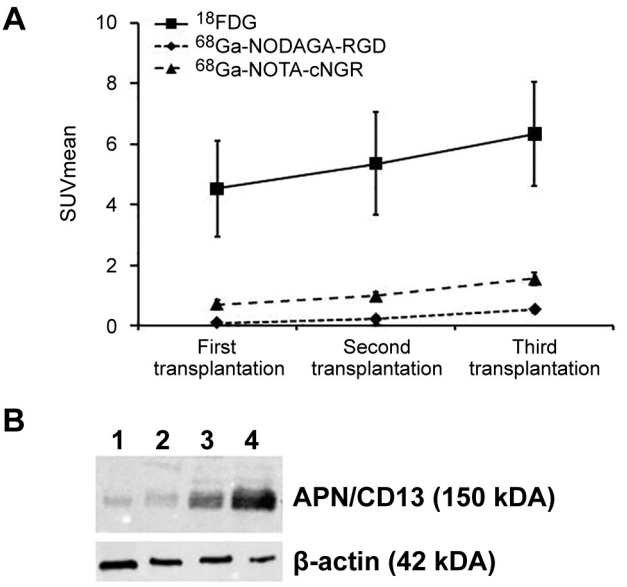

Figure 5. *Assessment of metastatic parathymic lymph nodes during serial transplantations. A panel: quantitative SUV analysis of radiotracer accumulation in the metastatic lymph nodes after serial transplantations. B panel: Western blot analysis of APN/CD13 expression in metastatic parathymic lymph nodes. 1: first series of lymph node experiments; 2: second series of lymph node experiments; 3: third series of lymph node experiments; 4: kidney (positive control).*

Exact knowledge of the molecular patterns of primary malignancies and their metastases may lead to changes in the existing therapeutic guidelines. The determination of the expression rate and localization of angiogenesis-associated molecules using specific radiopharmaceuticals would not only facilitate clinical trials of new drugs but could also be used in the selection of optimal treatment for individual patients. This might lay the foundation for individualized medicine.

Conclusion

In summary, considering all of the three series of experiments, the chemically induced rat-derived mesoblastic nephroma Ne/De tumors developing under the renal capsule were identified with all radiotracers applying *in vivo* PET imaging, while the thoracic metastases were unequivocally visualized only with [^{18}F]FDG and ^{68}Ga-NOTA-cNGR tracers. The steady increase in the accumulation of [^{18}F]FDG, ^{68}Ga-NODAGA-RGD, and ^{68}Ga-NOTA-cNGR in the tumors growing under the renal capsule and the thoracic parathymic lymph node metastasis could be observed during the serial transplantations. Therefore, the increase in glucose metabolism and the up-regulated expression of $\alpha_v\beta_3$ integrin and APN/CD13 molecules associated with neo-angiogenesis, which was observed in case of tumors and their metastases during the serial transplantations of the metastases, may indicated enhanced malignancy.

Conflicts of Interest

The Authors declare no conflicts of interest in relation to this study.

Authors' Contributions

JPSZ, ND, SzR, VA and AK: Visualization, investigation, conceptualization, writing original draft; JPSz, ND, AK, GO and GyT: Methodology, visualization, investigation; JPSZ: Validation; ZK, IK, ME and GM: Writing-reviewing and editing; ZK, IH and GyT: Writing-reviewing and editing.

Acknowledgements

The published work was supported by the EFOP-3.6.3-VEKOP-16-2017-00009 fund of European Union, by the NKFIH K119552 grant of the European Social Fund and National Research, Development and Innovation Office, and by the Thematic Excellence Programme (TKP2020-NKA-04) of the Ministry for Innovation and Technology in Hungary.

References

1 Soerjomataram I and Bray F: Planning for tomorrow: global cancer incidence and the role of prevention 2020-2070. Nat Rev Clin Oncol *18(10)*: 663-672, 2021. PMID: 34079102. DOI: 10.1038/s41571-021-00514-z

2 Lugano R, Ramachandran M and Dimberg A: Tumor angiogenesis: causes, consequences, challenges and opportunities. Cell Mol Life Sci *77(9)*: 1745-1770, 2020. PMID: 31690961. DOI: 10.1007/s00018-019-03351-7

3 Niccoli Asabella A, Di Palo A, Altini C, Ferrari C and Rubini G: Multimodality imaging in tumor angiogenesis: present status and perspectives. Int J Mol Sci *18(9)*: 1864, 2017. PMID: 28846661. DOI: 10.3390/ijms18091864

4 Melincovici CS, Boşca AB, Şuşman S, Mărginean M, Mihu C, Istrate M, Moldovan IM, Roman AL and Mihu CM: Vascular endothelial growth factor (VEGF) - key factor in normal and pathological angiogenesis. Rom J Morphol Embryol *59(2)*: 455-467, 2018. PMID: 30173249.

5 Takahashi S: Vascular endothelial growth factor (VEGF), VEGF receptors and their inhibitors for antiangiogenic tumor therapy. Biol Pharm Bull *34(12)*: 1785-1788, 2011. PMID: 22130231. DOI: 10.1248/bpb.34.1785

6 Su CY, Li JQ, Zhang LL, Wang H, Wang FH, Tao YW, Wang YQ, Guo QR, Li JJ, Liu Y, Yan YY and Zhang JY: The biological functions and clinical applications of integrins in cancers. Front Pharmacol *11*: 579068, 2020. PMID: 33041823. DOI: 10.3389/fphar.2020.579068

7 Ruoslahti E: Specialization of tumour vasculature. Nat Rev Cancer *2(2)*: 83-90, 2002. PMID: 12635171. DOI: 10.1038/nrc724

8 Beer AJ, Kessler H, Wester HJ and Schwaiger M: PET Imaging of integrin αVβ3 expression. Theranostics *1*: 48-57, 2011. PMID: 21547152. DOI: 10.7150/thno/v01p0048

9 Fukasawa K, Fujii H, Saitoh Y, Koizumi K, Aozuka Y, Sekine K, Yamada M, Saiki I and Nishikawa K: Aminopeptidase N (APN/CD13) is selectively expressed in vascular endothelial cells and plays multiple roles in angiogenesis. Cancer Lett *243(1)*: 135-143, 2006. PMID: 16466852. DOI: 10.1016/j.canlet.2005.11.051

10 Haubner R, Weber WA, Beer AJ, Vabuliene E, Reim D, Sarbia M, Becker KF, Goebel M, Hein R, Wester HJ, Kessler H and Schwaiger M: Noninvasive visualization of the activated alphavbeta3 integrin in cancer patients by positron emission tomography and [18F]Galacto-RGD. PLoS Med *2(3)*: e70, 2005. PMID: 15783258. DOI: 10.1371/journal.pmed.0020070

11 Decristoforo C, Hernandez Gonzalez I, Carlsen J, Rupprich M, Huisman M, Virgolini I, Wester HJ and Haubner R: 68Ga- and 111In-labelled DOTA-RGD peptides for imaging of alphavbeta3 integrin expression. Eur J Nucl Med Mol Imaging *35(8)*: 1507-1515, 2008. PMID: 18369617. DOI: 10.1007/s00259-008-0757-6

12 Pasqualini R, Koivunen E, Kain R, Lahdenranta J, Sakamoto M, Stryhn A, Ashmun RA, Shapiro LH, Arap W and Ruoslahti E: Aminopeptidase N is a receptor for tumor-homing peptides and a target for inhibiting angiogenesis. Cancer Res *60(3)*: 722-727, 2000. PMID: 10676659.

13 Trencsenyi G, Kertai P, Bako F, Hunyadi J, Marian T, Hargitai Z, Pocsi I, Muranyi E, Hornyak L and Banfalvi G: Renal capsule-parathymic lymph node complex: a new in vivo metastatic model in rats. Anticancer Res *29(6)*: 2121-2126, 2009. PMID: 19528472.

14 Dezso B, Rady P, Morocz I, Varga E, Gomba S, Poulsen K and Kertai P: Morphological and immunohistochemical characteristics of dimethylnitrosamine-induced malignant mesenchymal renal tumor in F-344 rats. J Cancer Res Clin Oncol *116(4)*: 372-378, 1990. PMID: 2143998. DOI: 10.1007/BF01612920

15 Máté G, Kertész I, Enyedi KN, Mező G, Angyal J, Vasas N, Kis A, Szabó É, Emri M, Bíró T, Galuska L and Trencsényi G: In vivo imaging of Aminopeptidase N (CD13) receptors in experimental renal tumors using the novel radiotracer (68)Ga-NOTA-c(NGR). Eur J Pharm Sci *69*: 61-71, 2015. PMID: 25592229. DOI: 10.1016/j.ejps.2015.01.002

16 Kis A, Dénes N, Szabó JP, Arató V, Jószai I, Enyedi KN, Lakatos S, Garai I, Mező G, Kertész I and Trencsényi G: In vivo assessment of aminopeptidase N (APN/CD13) specificity of different ^{68}Ga-labelled NGR derivatives using PET/MRI imaging. Int J Pharm *589*: 119881, 2020. PMID: 32946975. DOI: 10.1016/j.ijpharm.2020.119881

17 Berkel C and Cacan E: Metastases from metastases: comparative metastatic potential of human cancer cell lines originated from primary tumors or metastases in various tissues. J Cell Commun Signal *15(3)*: 461-464, 2021. PMID: 33861422. DOI: 10.1007/s12079-021-00617-3

18 Tait CR, Dodwell D and Horgan K: Do metastases metastasize? J Pathol *203(1)*: 515-518, 2004. PMID: 15095473. DOI: 10.1002/path.1544

19 Kis A, Szabó JP, Dénes N, Vágner A, Nagy G, Garai I, Fekete A, Szikra D, Hajdu I, Matolay O, Méhes G, Mező G, Kertész I and Trencsényi G: *In vivo* imaging of hypoxia and neoangiogenesis in experimental syngeneic hepatocellular carcinoma tumor model using positron emission tomography. Biomed Res Int *2020*: 4952372, 2020. PMID: 32832549. DOI: 10.1155/2020/4952372

Received May 14, 2022
Revised May 26, 2022
Accepted May 27, 2022